Available online at www.sciencedirect.com
SCIENCE DIRECT®
Catalysis Today 98 (2004) 423–429
CATALYSIS TODAY
www.elsevier.com/locate/cattod

Combinatorial synthesis and characterization of alkali metal doped oxides for diesel soot combustion

Hongmei An, Caitlin Kilroy, Paul J. McGinn*

Department of Chemical and Biomolecular Engineering, Center for Molecularly Engineered Materials, 182 Fitzpatrick Hall, University of Notre Dame, Notre Dame, IN 46556, USA

Available online 27 September 2004

Abstract

A polymerizable-complex powder synthesis method (PCM) was used in conjunction with automated solution deposition to generate combinatorial libraries of oxide powders doped with alkali metals. Chemical compositions were serially examined with automated thermogravimetric analysis for catalytic activity in the combustion of diesel soot. The relative soot combustion activity of $K_xLa_{1-x}FeO_3$, FeO_3, $A_{2x}Cu_{1-x}Fe_2O_4$ and $A_{2x}Co_{1-x}Fe_2O_4$ (A = Li, Na, K, Cs) are reported. In both of the alkali-metal doped systems, K was the best promoter of soot oxidation. In all three systems, K-rich samples in the ''mixed'' range ($x = 0.6$–0.9) generally show the lowest soot oxidation temperatures.

Keywords: Combinatorial synthesis; Oxide catalysts; Diesel soot combustion

1. Introduction

Due to health and environmental concerns related to particulate emissions from diesel engines, there is a need to develop technology to achieve reduced emission levels. In the United States, for example, the Environmental Protection Agency (EPA) has implemented new highway heavy-duty diesel engine emission standards. Among the technologies that are being considered to lower particulate emissions are regenerable traps. For such an application regeneration is accomplished by combustion of the collected particulate. In the absence of a catalyst, the filter must attain a minimum temperature in the range of 600–650 °C in air in order to auto-ignite and sustain the combustion. Catalyst-based diesel particulate filters are being considered in order to lower the required combustion temperatures. The focus of the present research is to employ a combinatorial processing/automated screening approach to systematically assess the efficacy of various oxides and related compounds in catalyzing diesel soot combustion.

1.1. Diesel soot combustion

The development of novel soot combustion catalysts have been reported in several recent studies [1–12]. Neeft et al. have shown that the nature of the contact (''loose'' or ''tight'') between the soot and the catalyst can affect the relative effectiveness of a catalyst in promoting soot oxidation [2]. Loose contact mode always shows reduced activity compared to tight contact mode for all compositions, but the degree of degradation varies from compound to compound. Milling of soot-catalyst mixtures yields ''tight'' contact, whereas in a particulate filter the soot-catalyst contact will typically be loose [3]. Thus, one strategy for catalyst development emphasizes the use of molten salts to assure good contact [4–6]. Industrial flame soot produced by high temperature pyrolysis (Printex-U from Degussa) has been shown to approximate diesel soot for laboratory experimental purposes [2]. Although the nature of diesel soot can vary with engine operating conditions, Printex-U has yielded good correlation with observations on actual soot.

The approach used in the present study emphasizes combinatorial catalyst processing. The combinatorial approach as applied to materials research uses parallel or

* Corresponding author. Tel.: +1 219 631 6151; fax: +1 219 631 8366.
E-mail address: pmcginn@nd.edu (P.J. McGinn).

0920-5861/$ – see front matter © 2004 Elsevier B.V. All rights reserved.
doi:10.1016/j.cattod.2004.08.006

automated serial processing and characterization of compounds in order to accelerate research and discovery. For catalyst development, it can allow the screening of large numbers of catalysts within short time periods. Several reviews of catalyst development provide in-depth background into the technology [13–20].

In previous work we have reported the use of the polymerizable-complex method (PCM) of powder processing combined with inkjet deposition for the combinatorial synthesis of complex oxide catalyst systems [21]. In PCM, also known as the Pechini method, metal ions are dissolved in solution with a chelating agent (citric acid) and a polyhydroxyl alcohol (ethylene glycol) [22]. The metal ions are chelated by the citric acid and are evenly distributed throughout the solution. Upon heating, the water or solvent evaporates, and the ethylene glycol undergoes polyesterification [23]. The result is a polymer resin with homogeneously distributed metal ions. The resin is subsequently decomposed at elevated temperatures to form the oxide powders. Because the PCM is a liquid mix process, metal ions are mixed on a molecular level, resulting in lower processing temperatures and shorter processing times than comparable solid-state processes. The oxide powders produced in this manner typically have higher surface areas than solid state processed powders.

In the approach used in the present study, inkjet dispensing technology is used to deposit PCM precursors combinatorially into TGA crucibles inserted into wells on a metal plate. The solutions are then reacted in parallel in a furnace, with the result being an array of oxide powders of varying composition. For soot combustion studies, the reaction step is followed by soot deposition. We report here the relative soot combustion activity of several series of perovskite and spinel structure compounds doped with alkali metals. Alkali metals have been shown to be effective at lowering the combustion temperature of carbon in air. One of the challenges for diesel soot exhaust filters is identifying alkali-doped compounds that are stable under the expected conditions that will be experienced in a soot combustion filter. In the present work we report on the soot oxidation behavior of several alkali-doped oxide systems.

2. Experimental procedures

2.1. Sample preparation

The PCM approach to powder synthesis was employed to generate the combinatorial libraries in this research. The precursor powders used were $Cu(NO_3)_2{\cdot}3H_2O$ (Johnson Matthey, Ward Hill, MA), $Ce(NO_3)_3{\cdot}6H_2O$ (Johnson Matthey), $Co(NO_3)_2{\cdot}H_2O$ (Johnson Matthey, Ward Hill, MA), $La(NO_3)_3{\cdot}6H_2O$ (Johnson Matthey, Ward Hill, MA), $Fe(NO_3)_3{\cdot}9H_2O$ (Johnson Matthey, Ward Hill, MA), $LiNO_3$ (Johnson Matthey, Ward Hill, MA), KNO_3 (Aldrich Chemical Company, St. Louis, MO), $NaNO_3$ (Aldrich Chemical Company) and $CsNO_3$ (Johnson Matthey, Ward Hill, MA). Each of these precursor powders was dissolved in distilled water to a concentration of 0.3 M to form the component solutions used in the drop-on-demand BioDot X/Y3200 printer (BioDot, Inc., Irvine, CA). Citric acid (Fisher Scientific) and ethylene glycol were dissolved in distilled water in a molar ratio of 60–40, which was previously determined to be the optimum ratio for this work [21]. The organic precursor solution was then dispensed along with metal nitrate solutions in the molar ratio of 38 metal to 62 organic.

A Biodot drop-on-demand printer is used for dispensing. It combines syringe pumps with inkjet dispensers, and incorporates a computer controlled x–y–z table. Libraries were dispensed into small TGA crucibles designed for this these studies. The crucibles are slightly taller (6 mm diameter $\times$ 6 mm high) than the crucibles normally used in the TGA in order to permit a larger volume of solution to be deposited. During deposition and processing, the crucibles rest in wells on a Hastelloy plate. Up to 55 different compositions can be deposited and processed in one run.

After deposition, each library is processed to form the final oxide powders. Libraries were heated in air slowly to 110 °C and held for 2 h to evaporate the solution and form the polymer resin. Libraries were heated to higher temperatures to decompose the polymer resin and form the final oxide powder.

2.2. Catalyst characterization

Simulated soot was prepared in a similar fashion to previous reports in the literature [5,24]. The soot used here is industrial flame soot manufactured by high-temperature pyrolysis (Printex® U carbon black, DeGussa AG, Dusseldorf, Germany). The reaction properties of the Printex® U have been determined to be chemically similar to that of actual diesel exhaust soot [24]. The soot was suspended in methanol at a concentration of 1.5% by weight and briefly ultrasonicated. The soot suspension was manually pipetted, as it proved difficult to clean completely from the inkjet dispensing system. The soot solution was allowed to dry on the powders at 90 °C for 10 min prior to TGA characterization.

Soot/catalyst mixtures, in a weight ratio of approximately 1:9, were characterized serially in an auto-loading high resolution modulated TGA (TA Instruments 2950). Oxygen was used as reaction gas, with the balance and furnace gas flow set at 80 and 120 ml/min, respectively. All of the data shown in this work were repeated at least one time and the results are reproducible. The error for ignition temperature is ±5 °C. Precise control of the catalyst synthesis conditions (composition, reaction and calcination temperature) and the soot/catalyst ratio is very important to achieve reproducibility. X-ray diffraction was performed using a Scintag X1 powder diffractometer (Thermo Corp. Waltham, MA) to verify phase formation as a function of composition.

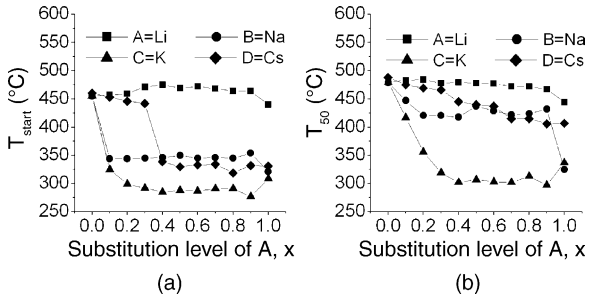

Fig. 1. TGA results for freshly prepared oxides $A_{2x}Cu_{1-x}Fe_2O_4$ (A = Li, Na, K, Cs): (a) soot combustion onset temperature (T_{start}) vs. composition; (b) the temperature at which half of the soot has been oxidized (T_{50}) vs. composition.

3. Results and discussion

3.1. $A_{2x}Cu_{1-x}Fe_2O_4$

TGA results for compounds in the series $A_{2x}Cu_{1-x}Fe_2O_4$ (A = Li, Na, K, Cs) are shown in Fig. 1a. These compounds were all synthesized at 650 °C. Fig. 1 shows the onset temperature where combustion starts (T_{start}), while Fig. 1a shows the temperature corresponding to when half of the carbon has been oxidized (T_{50}) as a function of composition for the various dopants. Both plots show the results for freshly prepared catalyst run for the first time. It is evident that overall dopant ranking relative to their effect on soot combustion temperature is K > Cs ∼ Na > Li. This tendency is similar to the results reported by Shangguan et al. [25]. They studied the effect of alkali doping of $CuFe_2O_4$ ($A_{0.1}Cu_{0.9}Fe_2O_4$, A = Li, Na, K, Cs) on the simultaneous removal of NO_x-soot. Even though there is some difference in the soot oxidation mechanism in NO_x gas flow compared to air flow, they found that the activity of alkali metal doped oxides increased with atomic number as K ∼ Cs > Na ≫ Li. NO_x is a much stronger oxidant than O_2, so the soot ignition temperatures reported by Shangguan are lower than those seen in this study.

Small amounts of both Na and K lead to a decrease in $T_{start} > 100$ °C. A noticeable drop in T_{start} with Cs doping is not observed until the level exceed $x > 0.3$. Examination of the T_{50} values shows that K additions are much more active

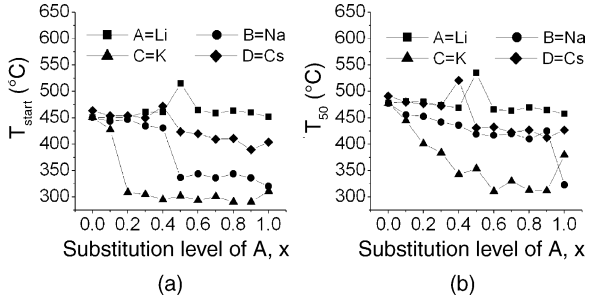

Fig. 2. Results of the second TGA run of $A_{2x}Cu_{1-x}Fe_2O_4$ (A = Li, Na, K, Cs) oxides. (a) T_{start} vs. composition; (b) T_{50} vs. composition.

than Cs, Na or Li in $A_{2x}Cu_{1-x}Fe_2O_4$ compound, with T_{50} values of ∼300 °C existing over a wide range of substitution (x = 0.4–0.9).

After the first run through the TGA, these samples had soot solution deposited on them again; they were dried, and again characterized in the TGA to assess their relative stability. Fig. 2a and b shows the TGA data for the second run of these compounds. Again the K-doped samples are the most active. The precipitous drop in T_{start} with composition does not begin until $x = 0.2$ for the K-doped samples, but this change is much less than in the Na-doped samples, where the drop moves from $x = 0.1$ (fresh) to $x = 0.5$. The T_{50} values also show the K-doped sample is the most active, although the lowest temperatures now are in the x = 0.6–0.9 range. Fig. 3 shows the relative stability of the T_{start} and T_{50} behavior after the first and second runs, along with the values observed after the samples were exposed to the laboratory ambient for a period of 1 week for both Na (Fig. 3a) and K (Fig. 3b) doping. The 1 week exposure is a relatively simple way to assess the level of hygroscopic behavior. In some alkali metal-doped systems, we have observed substantial stability problems. Exposure to laboratory air leaves the $Na_{2x}Cu_{1-x}Fe_2O_4$ compound relatively unchanged, with T_{50} values in the 420–440 °C range from x = 0.3 to 0.9. The lowest value (∼380 °C) is seen for the Na = 1.0 sample ($Na_2Fe_2O_4$). The K-doped samples show much greater variability in their T_{50} values, with the most stable composition (and lowest T_{50} value after 1 week in air of ∼325 °C) being at $x = 0.7$.

Powder diffraction data for the $K_{2x}Cu_{1-x}Fe_2O_4$ substitution series (processed at 650 °C for 3 h) are summarized

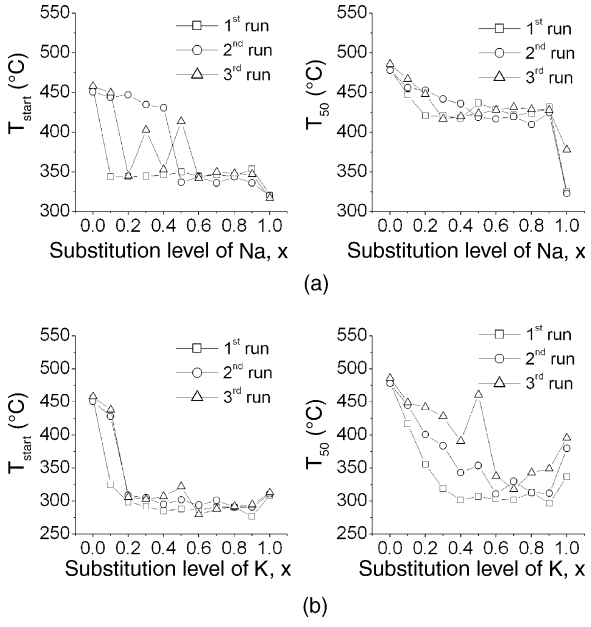

Fig. 3. T_{start} and T_{50} TGA soot combustion stability results of catalysts (a) $Na_{2x}Cu_{1-x}Fe_2O_4$ and (b) $K_{2x}Cu_{1-x}Fe_2O_4$. Results are shown as freshly prepared (“first run”), second run and after exposure to laboratory ambient for 1 week.

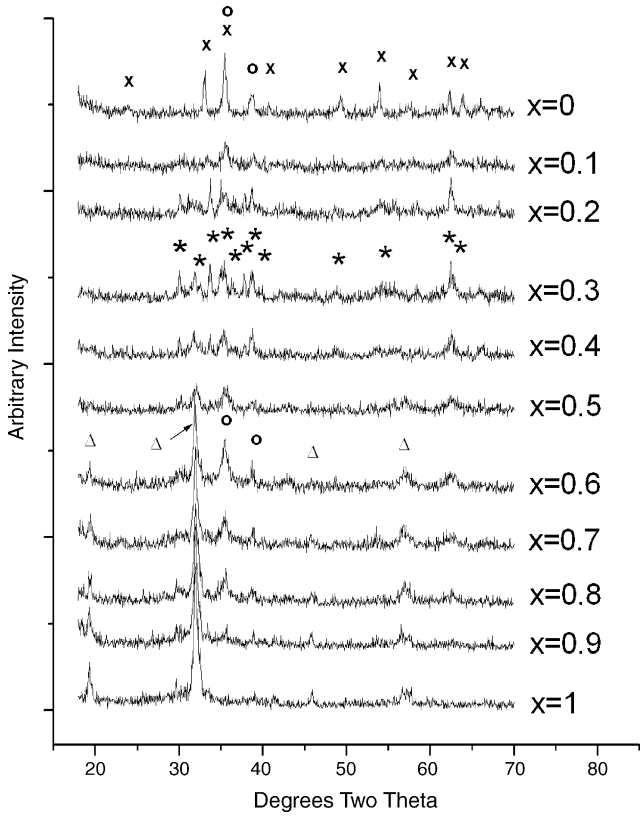

Fig. 4. XRD patterns for $K_{2x}Cu_{1-x}Fe_2O_4$, with likely peak phase assignments: ((○) denotes CuO peaks(ICDD Card No: 45-0135); (×) denotes Fe_2O_3 peaks (ICDD Card No: 33-0664); (✱) denotes $K_2Fe_{10}O_{16}$ peaks (ICDD Card No: 40-0135); (△) denotes $KFeO_2$ peaks (ICDD Card No: 83-2153)).

in Fig. 4. The likely phases are marked in the patterns. The compounds that exhibit the best properties (i.e. $x > 0.6$) all show strong $KFeO_2$ (ICDD 83-2153) lines. There is significant overlap between CuO and $KFe_{10}O_{16}$, so it is difficult to unambiguously determine if there is any remaining trace $KFe_{10}O_{16}$ in the $x > 0.6$ range, but there seems to be primarily $KFeO_2$ and CuO ((ICDD 45-0135)). It seems logical to attribute the superior soot combustion activity to the presence of $KFeO_2$, but solely on that basis one would expect to see the best properties for the $x = 1.0$ composition Instead, samples in the "mixed" range show the lowest combustion temperatures and the best stability.

3.2. $A_{2x}Co_{1-x}Fe_2O_4$

Fig. 5 shows TGA results for the first run of samples in the system $A_{2x}Co_{1-x}Fe_2O_4$ (A = Li, Na, K, Cs). As in the above cases, these compounds were all synthesized at 650 °C. Fig. 5a shows the T_{start} values, while Fig. 5b shows the T_{50} values as a function of composition for the various dopants. Similar to what was observed in the doped $CuFe_2O_4$, the K- and Na-doped compounds are again the most active for soot combustion, with K > Na > Cs ~ Li. As before, small amounts of either Na or K lead to noticeable

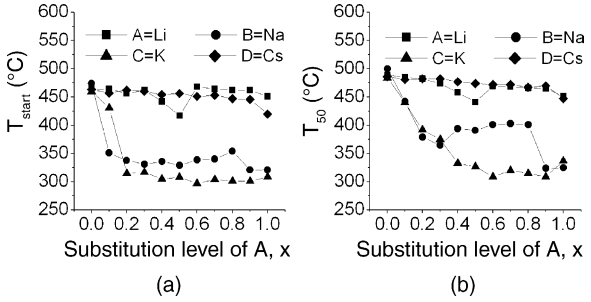

Fig. 5. TGA results for freshly prepared oxides $A_{2x}Co_{1-x}Fe_2O_4$ (A = Li, Na, K, Cs): (a) T_{start} vs. composition; (b) T_{50} vs. composition.

decrease in T_{start} of the order of 100 °C. The T_{start} temperature drop occurs at lower doping levels with Na than K. Neither Cs nor Li doping show significant effects on T_{start}. The T_{50} values shows that K additions are more active than Na in $A_{2x}Cu_{1-x}Fe_2O_4$ at levels of $x = 0.4$ and above. At doping levels between $x = 0.6$ and 0.9 the best T_{50} values (around 325 °C) are obtained.

The results from the second soot combustion cycle in the TGA for $A_{2x}Co_{1-x}Fe_2O_4$ (A = Li, Na, K and Cs) are shown in Fig. 6. As with the first run, the K-doped T_{start} values (Fig. 6a) are slightly lower than the Na-doped samples at doping levels of $x = 0.2$ or greater. However, the T_{50} values (Fig. 6b) of the sodium doped samples are slightly lower (better) than the K-doped samples at all compositions except around $x =$ 0.6–0.7, where they are approximately equal. The doped $CoFe_2O_4$ compounds were allowed to sit in the lab ambient for a week and retested. The T_{50} stability of the Na- and K-doped compounds are shown in Fig. 7a and b, respectively. Both compounds show a loss of activity, with the $x = 0.6$–0.9 K-doped sample showing the best properties, with T_{50} values of ~360 °C, 20 °C lower than the best Na-doped sample (at $x = 1$).

Powder diffraction data for the $K_{2x}Co_{1-x}Fe_2O_4$ substitution series (processed at 650 °C for 3 h.) showed only $CoFe_2O_4$ (ICDD 22-1086) was obtained for $x = 0$ and $KFeO_2$ (ICDD 83-2153) for $x = 1.0$. For the Co-rich samples, $CoFe_2O_4$ (ICDD 22-1086) is the dominant phase; while for substitution levels greater than $x > 0.6$, the dominant lines are from $KFeO_2$ (ICDD 83-2153). Unlike the counterpart Cu containing system, this system does not show evidence of a

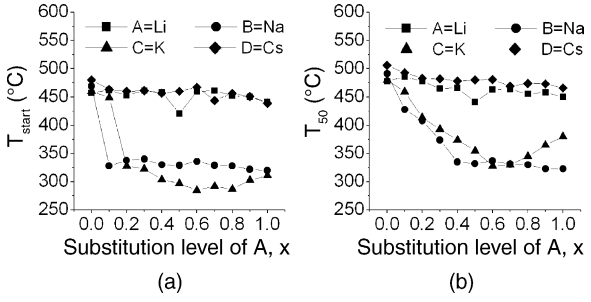

Fig. 6. Results of the second TGA run of $A_{2x}Co_{1-x}Fe_2O_4$ (A = Li, Na, K, Cs) oxides. (a) T_{start} vs. composition; (b) T_{50} vs. composition.

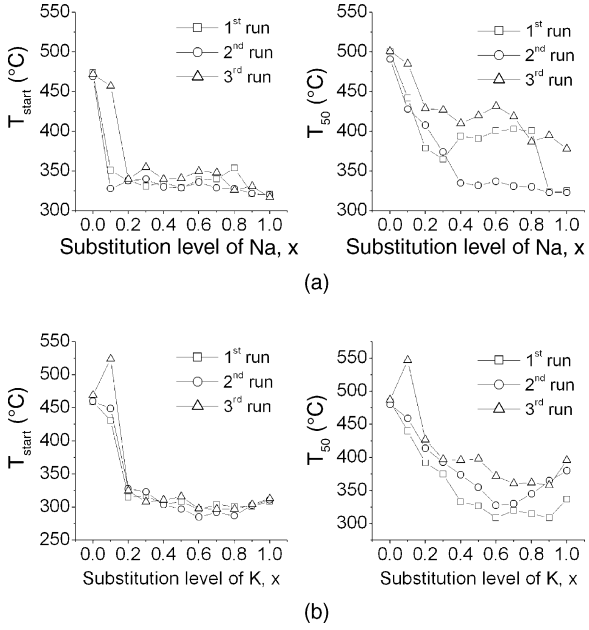

Fig. 7. T_{start} and T_{50} TGA soot combustion stability results of catalysts (a) $Na_{2x}Co_{1-x}Fe_2O_4$ and (b) $K_{2x}Co_{1-x}Fe_2O_4$. Results are shown as freshly prepared ("first run"), second run and after exposure to laboratory ambient for 1 week.

cobalt oxide phase at $x > 0.6$ values, but rather the trace phase seems to be a K-substituted $CoFe_2O_4$ phase.

3.3. $K_xLa_{1-x}FeO_3$

Based on the data shown above, it is evident that K-containing compounds offer strong possibilities as potential soot oxidation catalysts. Thus, the $K_xLa_{1-x}FeO_3$ system was examined as another possible catalyst to enhance soot oxidation. The TGA behavior is summarized in Fig. 8. For the fresh samples $K_xLa_{1-x}FeO_3$ (first run), T_{50} drops from 510 to 300 °C with an increase of K content and remains nearly constant for $x \geq 0.5$. The T_{start} and T_{50} values, respectively, for the first and second TGA runs, and after 1 week of exposure to laboratory ambient, are shown in Fig. 8a and b. It was found $K_xLa_{1-x}FeO_3$ ($x > 0.1$) can ignite soot at about 300 °C and the sample with $0.3 \leq x \leq 0.9$ can ignite soot below 350 °C, even after two reaction cycles and being

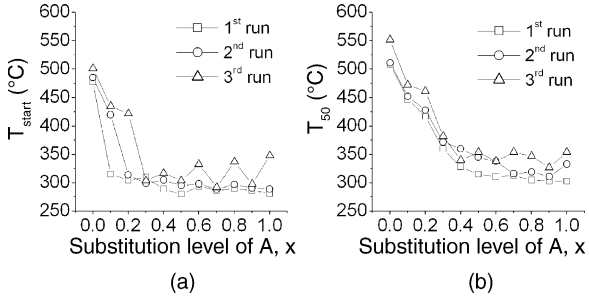

Fig. 8. T_{start} and T_{50} TGA soot combustion stability results of $K_xLa_{1-x}FeO_3$. Results are shown as freshly prepared ("first run"), second run and after exposure to laboratory ambient for 1 week.

exposed to laboratory air for 1 week. The T_{50} values are roughly unchanged (~325 °C) at values of $x > 0.50$. There is some decrease in activity with 1 week exposure to laboratory ambient, but T_{50} values around 350 °C are still observed. Fino et al. reported that, the T_p (temperature corresponding to the peak in the CO_2 exhaust concentration) is about 520 °C when $LaFeO_3$ is used as catalyst for soot combustion [26], which agrees fairly well with our T_{50} observation. It should be noted that their test conditions (air flow: 100 ml/min, heating rate: 5 °C/min, soot/catalyst = 1:9 weight ratio) were similar to those used in the present work. Their study involved a series of $LaMO_3$ compounds (M = Cr, Fe, Mn). In $LaCrO_3$ (the compound showing the best behavior) K doping ($La_{0.9}K_{0.1}Cr_{0.9}O_{3-\delta}$) led to improved soot combustion behavior, exhibiting soot ignition well below 400 °C. Teraoka et al. also investigated $La_{0.9}K_{0.1}FeO_3$ and reported it can ignite diesel soot at 276 °C in NO + O_2 environment [27]. Unfortunately, neither study examined systematic K doping of $LaFeO_3$, as in the present study.

All of the samples in the $K_xLa_{1-x}FeO_3$ series (except for $x = 0$) show multiple stages in the TGA curves, examples of which are shown in Fig. 9. For example, three stages of soot combustion are observed in the TGA curve for $x = 0.5$ (Fig. 9 inset). The three stages represent catalytic soot combustion occurring with different reaction rates (carbon wt.% (°C)) as indicated by the changing slopes of the weight loss curves. In contrast, the TGA curve for $x = 0$ shows only one soot combustion rate in the 450–550 °C temperature range, as indicated by the constant slope over the weight loss portion of the curve. The type of stepped behavior shown by all of the curves except $x = 0$ is typically related to the existence of multiple phases in a sample.

Powder X-ray diffraction results shown in Fig. 10 $LaFeO_3$ is essentially the only phase at $x < 0.5$. At higher K substitution levels (beginning at $x = 0.6$) other phases are present, including $K_6Fe_2O_6$ and FeO_x. With increased K

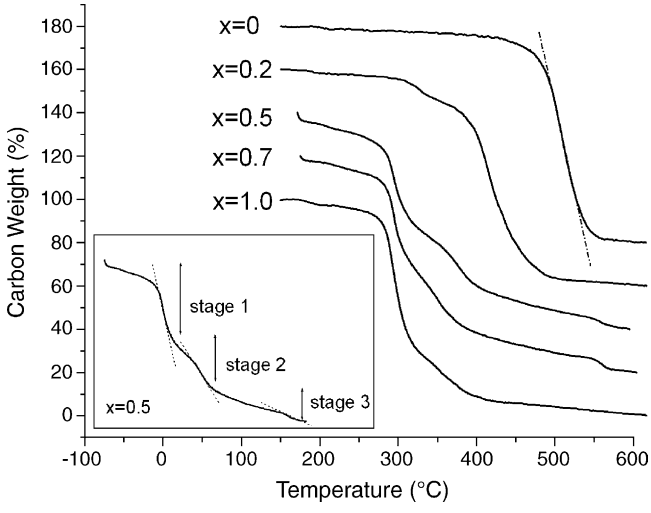

Fig. 9. Representative TGA curves of soot combustion in O_2 flow for freshly prepared $K_xLa_{1-x}FeO_3$ ($x = 0$, 0.2, 0.5, 0.7 and 1.0). All curves except $x = 0$ show several steps.

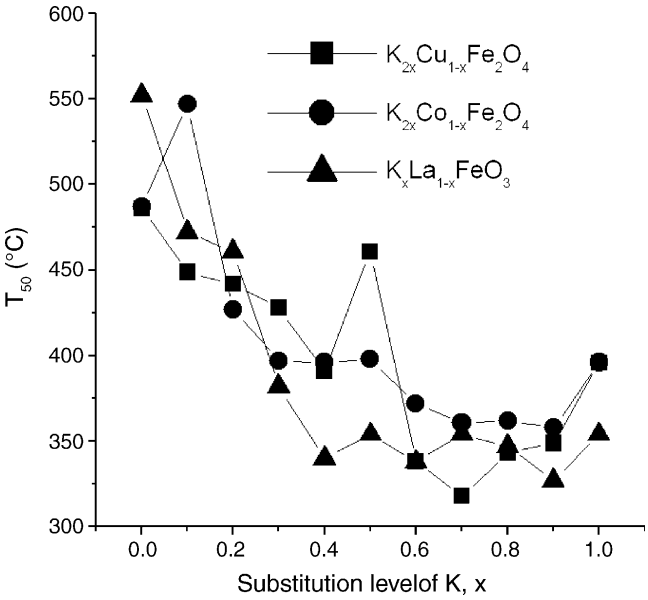

Fig. 10. The comparison of 1 week aged T_{50} temperatures as a function of composition for 3 K-substituted systems: $K_{2x}Co_{1-x}Fe_2O_4$, $K_{2x}Cu_{1-x}Fe_2O_4$ and $K_xLa_{1-x}FeO_3$ determined by TGA.

substitution levels, the lattice parameter of the $LaFeO_3$ shifts, as evidenced by the change in its peak positions to progressively lower 2θ values. At $x = 1$, KFe_2O_6 was not obtained, unlike the case for the $K_{2x}Co_{1-x}Fe_2O_4$ and $K_{2x}Cu_{1-x}Fe_2O_4$ systems. In those cases the powder was reacted at 650 °C, yielding pure $KFeO_2$. However, the $K_xLa_{1-x}FeO_3$, powder was prepared at 600 °C. At this temperature kinetic limitations might have delayed formation of $KFeO_2$. Instead a mixture of several potassium and iron oxides and hydroxides are seen in the diffraction data.

The XRD data supports the explanation that the multiple stages of weight loss seen in the TGA curves for $x \geq 0.5$ are due to the presence of several phases in the sample. However, for samples with $0 < x < 0.5$, the XRD patterns only clearly show one phase, $LaFeO_3$, being present.

There are number of possible causes for presence of multiple steps in the TGA soot decomposition curves including: (1) a combination of different phases (catalysts), causing soot combustion at different temperatures and reaction rates; (2) varying soot/catalyst contact, in which case the soot contacting the catalysts less directly (e.g. ''loose'' contact) will react at higher relative temperatures than soot with intimate catalyst contact; (3) continued decomposition of the catalysts, such that some of the apparent weight loss is not due to soot combustion.

We have examined the soot contact issue by looking at soot combustion on single phase, commercial catalysts (CuO, Fe_2O_3, Fe_3O_4, and CeO_2) and multi-stage weight changes have not been found for any pure catalysts. Thus, it is thought that the method used to mix the soot and catalysts and the soot/catalyst ratio used in our research can provide intimate, uniform soot/catalyst mixing, eliminating possibility (2) as the cause of the multiple steps.

In using the Pechini process as employed in this work it is possible that minimizing the reaction temperature in an effort to maximize particle surface area can lead to incompletely reacted precursors. In this case one might see continued decomposition during soot combustion analysis. In an effort to clarify this issue, the catalysts x = 0–0.4 were run *without soot* in the TGA using the same temperature schedule as during soot combustion. There was no obvious decomposition weight loss found, suggesting that possibility (3) is not responsible for the multiple steps.

This leaves the presence of multiple phases as the most likely possibility. Typically, the detection limit in powder X-ray diffraction is on the order of a few percent. For Pechini processing, lower limit detection is further impaired because powder prepared by the Pechini method and calcined at low temperatures results in very fine particles which yield broad, lower intensity peaks in powder diffraction. Thus, it is possible that the trace impurity cannot be detected by XRD, but still yields an effect during thermal analysis. This is not unlike the case in processing of the high temperature superconductor $YBa_2Cu_3O_7$, where the presence of the trace phase $BaCuO_2$ is not seen in powder XRD, but is readily apparent by differential thermal analysis [28].

Thus, we believe there are trace addition phases that are below the detection limit of the powder diffractometer that are responsible for the multiple steps in the TGA data.

In order to compare the three systems considered here, Fig. 10 shows the T_{50} curves of the 1 week ''aged'' samples for $K_{2x}Co_{1-x}Fe_2O_4$, $K_{2x}Cu_{1-x}Fe_2O_4$ and $K_xLa_{1-x}FeO_3$. These are replotted data from earlier figures. The systems are all fairly similar in their behavior, in that they all exhibit their best properties in the x = 0.6–0.9 range. In the case of $K_{2x}Cu_{1-x}Fe_2O_4$ and $K_{2x}Co_{1-x}Fe_2O_4$, both contain $KFeO_2$ along with a secondary phase (CuO or $CoFe_2O_4$). In the $K_xLa_{1-x}FeO_3$ system, the K substituted $LaFeO_3$ is the dominant phase with small amounts of $K_6Fe_2O_6$ and FeO_x. Enough is not understood about the catalysis mechanism in these systems to explain the role of the second phases. This will be the focus of further studies. However, they clearly are important in that the best properties uniformly occur in the 2-phase composition regions.

The cause of the run-to-run variation seen in many of the samples (Figs. 3, 7 and 8) is unclear at present. It may be due to the loss of alkali-earthi ions at high temperature. We have seen some evidence of potassium loss, for example, with repeated cycling or extended periods in the 500–700 °C range. This is the focus of on-going studies.

Previous work has shown that the soot/catalyst contact resulting from the preparation method used in this work is between the extremes of ''loose'' and ''tight'' [29]. The loosest contact is seen when the soot is dusted onto the catalyst, while tightest contact results from intimate milling of the soot and catalyst. The contact produced by suspending the soot in methanol is thought to represent a reasonable approximation of the contact observed in an actual soot filter.

The use of TGA offers a reliable technique for characterization of catalyst activity for soot combustion. The biggest disadvantage of this approach is that it is relatively slow, with characterization of individual compositions requiring approximately 75 min each (ramping up to ~650 °C and cooling back to room temperature). However, because it is automated, the system can run unattended. The advantages auto-TGA offers are significant, especially in terms of repeatability and consistency. In addition, results generated can be directly compared with the results of other groups (particle size, soot contact differences, etc., notwithstanding). The degree of soot/catalyst contact is highly repeatable, and not unlike actual filter conditions.

For samples exhibiting favorable behavior (i.e. a "hit") soot can be re-deposited and the sample can be run again. In fact, we have used this method to observe the slow loss of activity of a catalyst. The TGA can show the deactivation of a sample very clearly by an increase of ignition temperature, a drop of reaction rate, etc. On the other hand, if a catalyst slowly becomes more active over an extended period, it is likely that TGA studies as performed here (i.e. not re-characterizing the entire library multiple times) might miss such behavior. In the present studies all of the samples were run three times in the TGA, with fresh catalyst being tested in the first run, and "used" catalysts in the second run. A third test was performed after the samples were exposed to the laboratory ambient for a period of 1 week to test the hygroscopic behavior of catalysts. This is the emphasis of our future work.

4. Conclusions

A combinatorial study was performed to examine the effect of alkali doping of $CuFe_2O_4$, and $CoFe_2O_4$, and K doping of $LaFeO_3$, on their diesel soot combustion properties. For $A_{2x}Cu_{1-x}Fe_2O_4$ the overall dopant ranking relative to their effect on soot combustion temperature is K > Cs ~ Na > Li. For $A_{2x}Co_{1-x}Fe_2O_4$, the K- and Na-doped compounds are again the most active for soot combustion, with a general activity trend of K > Na > Cs ~ Li. In all three systems considered, the best soot combustion properties were in the x = 0.6–0.9 range, where there were multiphase samples.

Acknowledgements

This study was supported in part by The Indiana 21st Century Research & Technology Fund, Petroleum Research Foundation (PRF# 37571-AC5) and Cummins, Inc.

References

[1] G. Mul, J.P.A. Neeft, O.P. van Pruissen, M. Makkee, J.A. Moulijn, Appl. Catal. B: Environ. 1 (1992) 117.
[2] J.P.A. Neeft, M. Makkee, J.A. Moulijn, Appl. Catal. B: Environ. 8 (1996) 57.
[3] J.P.A. Neeft, O.P. van Pruissen, M. Makkee, J.A. Moulijn, Appl. Catal. B: Environ. 12 (1997) 21.
[4] B.A.A.L. van Setten, J. Bremmer, S.J. Jelles, M. Makkee, J.A. Moulijn, Catal. Today 53 (1999) 613.
[5] S.J. Jelles, B.A.A.L. van Setten, M. Makkee, J.A. Moulijn, Appl. Catal. B: Environ. 21 (1999) 35.
[6] G. Saracco, N. Russo, M. Ambrogio, C. Badini, V. Specchia, Catal. Today 60 (2000) 33.
[7] G. Neri, L. Bonaccorsi, A. Donato, C. Milone, M.G. Musolino, A.M. Visco, Appl. Catal. B: Environ. 11 (1997) 217.
[8] C.A. Querini, M.A. Ulla, F. Requejo, J. Soria, U.A. Sedran, E.E. Mire, Appl. Catal. B: Environ. 15 (1998) 5.
[9] A. Bellaloui, J. Varloud, P. Meriaudeau, V. Perrichon, E. Lox, M. Chevrier, C. Gauthier, F. Mathis, Catal. Today 29 (1996) 421.
[10] C. Badini, G. Saracco, N. Russo, V. Specchia, Catal. Lett. 69 (2000) 207.
[11] G. Saracco, N. Russo, M. Ambrogio, C. Badini, V. Specchia, Catal. Today 60 (2000) 33–41.
[12] G. Saracco, C. Badini, N. Russo, V. Specchia, Appl. Catal. B: Environ 21 (1999) 233.
[13] B. Jandeleit, D.J. Schaefer, T.S. Powers, H.W. Turner, W.H. Weinberg, Angew. Chemie Intl. Ed. 38 (1999) 2495.
[14] A. Hagemeyer, B. Jandeleit, Y. Liu, D.M. Poojary, H.W. Turner, A.F. Volpe Jr., W.H. Weinberg, Appl. Catal. A: Gen. 221 (2001) 23.
[15] X.-D. Xiang, X. Sun, G. Briceño, Y. Lou, K.-A. Wang, H. Chang, W.G. Wallace-Freedman, S.-W. Chen, P.G. Schultz, Science 268 (1995) 1738.
[16] R.B. van Dover, L. Schneemeyer, R.M. Fleming, Nature 392 (1998) 162.
[17] X.-D. Sun, K.-A. Wang, Y. Yoo, W.G. Wallace-Freedman, C. Gao, X.-D. Xiang, P.G. Schultz, Adv. Mater. 9 (1997) 1046.
[18] E. Reddington, A. Sapienza, B. Gurau, R. Viswanathan, S. Sarangapani, E.S. Smotkin, T.E. Mallouk, Science 280 (1998) 1735.
[19] A. Holzwarth, H.-W. Schmidt, W.F. Maier, Angew. Chemie Int. Ed. 37 (1998) 2644.
[20] P. Cong, R.D. Doolen, Q. Fan, D.M. Giaquinta, S. Guan, E.W. McFarland, D.M. Poojary, K. Self, H.W. Turner, W.H. Weinberg, Angew. Chemie Int. Ed. 38 (1999) 791.
[21] H.M. Reichenbach, P.J. McGinn, J. Mater. Res. 16 (2001) 967.
[22] M. Pechini, US Patent 3,330,697 (1967).
[23] M. Kakihana, M. Yoshimura, Bull. Chem. Soc. Jpn. 72 (1999) 1427.
[24] J.P.A. Neeft, Ph.D. Thesis, Delft University of Technology, 1995.
[25] W.F. Shangguan, Y. Teraoka, S. Kagawa, Appl. Catal. B: Environ. 16 (1998) 149.
[26] D. Fino, N. Russo, G. Saracco, V. Specchia, J. Catal. 217 (2003) 367.
[27] Y. Teraoka, K. Nakano, W.F. Shangguan, S. Kagawa, Catal. Today 27 (1996) 107.
[28] U. Balachandran, R.B. Poeppel, J.E. Emerson, S.A. Johnson, M.T. Lanagan, C.A. Youngdahl, D.L. Shi, K.C. Goretta, N.G. Eror, Mater. Lett. 8 (1989) 454.
[29] H.M. Reichenbach, Studies of the Combinatorial Synthesis of Catalyst Oxide Powders, Ph.D. Thesis, University of Notre Dame, April, 2002.